Journal of Physical Chemistry and Functional Materials

Home Page of Journal: https://dergipark.org.tr/jphcfum

Determination of Three Metal Ions (Cu^{+2}, Pb^{+2}, Cd^{+2}) by Ultraviolet-visible Spectroscopy

Sarbaz Mohammed Qader[1], Azhin hamad mohammed[2], Akar Mahmood Muhammed[3], Rebaz Anwar Omer[1, 4]*, Aryan Fathulla Qader[1]

[1]*Department of Chemistry, Faculty of Science and Health, Koya University, Danielle Mitterrand Boulevard, Koya KOY45, Kurdistan Region - F.R. Iraq.*

[2]*Department of Physics, Faculty of Science and Health, Koya University, Danielle Mitterrand Boulevard, Koya KOY45, Kurdistan Region - F.R. Iraq.*

[3]*Chemistry Department, College of Science, University of Raparin, Rania, 46012, Sulaymaniyah, Iraq*

[4]*Department of Pharmacy, College of Pharmacy, Knowledge University, Erbil 44001, Iraq*

**Corresponding author: E-mail: rebaz.anwar@koyauniversity.org*

ABSTRACT

This review article focuses on determining the concentration of trace metal ions using Ultraviolet-visible (UV-Vis) spectrophotometry, a technique widely recognized for its effectiveness in both qualitative and quantitative analysis of environmental pollutants, particularly in water samples. The study specifically examines three metal ions: Cu^{2+}, Pb^{2+}, and Cd^{2+}. When analyzed independently, their maximum absorption wavelengths (λ-max) are recorded at 755 nm, 100-380 nm, and 323.9 nm, respectively. However, upon interaction with a reagent, the λ-max values shift, demonstrating the effect of complex formation or other chemical interactions on the absorption properties of these ions. UV-Vis spectrophotometry measures the absorption of light in the near ultraviolet to visible range (200-400 nm), making it a suitable method for detecting and quantifying trace amounts of metal ions in water. The methodology involves constructing calibration curves based on the absorption spectra, which allows for the correlation of specific absorption bands with the concentrations of metal ions in the sample. This technique is essential for pharmaceutical analysis, where it is used to determine the identity, strength, quality, and purity of chemical substances. In addition to the experimental analysis, the article provides a bibliometric overview, classifying the top 10,000 cited UV-Vis spectrophotometry papers from 2016-2017 into four key research clusters: nanoparticles, photocatalysis, crystals, and biological interactions, particularly those involving silver (Ag) and gold (Au) nanoparticles.

ARTICLE INFO

Keywords:

Ultraviolet-visible spectroscopy
Metal ion, Beer's
Lambert's Law

Received: 2024-08-18
Accepted: 2024-10-02
ISSN: 2651-3080
DOI: 10.54565/jphcfum.1535225

1. Introduction

The first spectroscopic scientist was Johannes Marcus Marci of Kronland, Eastern Bohemia, who flourished from 1595 until 1667. He experimented in an attempt to explain why rainbows arise. In 1648, he also penned a book called The Book of Thaumas, in which he covered a variety of related subjects like the nature of the colors that occur and the origins of the Heavenly Rainbow. The word "spectrum" was used by Isaac Newton to describe how the sun's white light might be divided into an infinite variety of colors [1]. The inaugural commercial spectrophotometer, the Beckman DU, was launched by Beckman in 1941. The initial use is quantifying vitamins A and D to determine their overall concentration in diverse sources. The subsequent generation, the Beckman DR, was launched in 1953. In 1960, kinetic experiments on several compounds were conducted utilizing UV-Visible spectrophotometers [2].

When molecules, atoms, or ions in a sample transition from one energy state to another, they absorb and emit electromagnetic radiation (EMR), which is measured and interpreted in spectroscopy [3]. UV-VIS Spectroscopy: This technique operates on the principle that the absorbance of a solution is directly proportional to the

concentration of the absorbing species and the path length. Ultraviolet (UV) spectroscopy is a physical method of optical spectroscopy that utilizes light in the visible, ultraviolet, and near-infrared spectra. Consequently, it can be utilized to determine the absorber concentration in a solution for a particular path length. Given that UV-VIS spectroscopy has been extensively utilized for 37 years and has become the paramount analytical instrument in contemporary laboratories, it is crucial to comprehend the relationship between absorbance and concentration variation. Alternative approaches may be used in various contexts; however, none surpass UV-VIS spectroscopy regarding user-friendliness, versatility, precision, rapidity, and cost-effectiveness [4, 5].

Among the several heavy metals, lead (Pb), cadmium (Cd), mercury (Hg), chromium (Cr), and arsenic (As) are the most poisonous. Additionally, even little amounts of these extremely hazardous Metals may not be beneficial to human health and the environment. The main ways that humans are exposed to these metal ions are through food, drink, and the air. Fish is the main source of exposure to mercury. Moreover, heavy metals are thought to be among the most harmful water contaminants since they harm both the health of humanity and the environment. Finding these ions of heavy metals and their concentrations in drinking and natural water sources is crucial [6, 7]. One of the earliest instrumental analysis techniques, UV-VIS spectrometry serves as the foundation for several optimal approaches for determining the semi-micro and micro amounts of analytics within an sample. It measures the effects of electromagnetic energy in the visible and UV spectrum on absorbed entities such as molecules, atoms, or ionized. The interaction with electromagnetic energy in the UV/Visible area and ions, molecules, or compounds produces the UV-VIS spectrum [2, 8, 9]. It serves as the foundation for the investigation of several compounds, including, organic, inorganic, and Molecular biology. These conclusions include usage in industry, research, hospitals, and the chemical examination of samples from the environment. It is therefore important to learn about the origin of the UV-VIS spectrum and its characteristics [10]. Ultraviolet (UV), visible (Vis) and near infrared (NIR) spectroscopy in the electromagnetic spectrum region is also referred to as electronic spectroscopy since, Electrons in a substance shift from low-level energy to high-level energies atomic or molecular orbitals when exposed to light [11]. Transition metal ions (d-d transitions and ligand-to-metal or metal-to-ligand charge transfer transitions) may be the site of such electron transfer processes, and both organic and inorganic compounds (mostly transitions between ($n \rightarrow \pi^*$ and $\pi \rightarrow \pi^*$). They bear the blame for the matter's color [5, 12].

Several labs for biochemistry and microbiology, UV/VIS Analysis using spectrophotometry is essential. It is used to measure protein levels in solutions, as well as to identify microorganisms and determine the kinetics of enzymes in pharmaceutical goods [13]. Being a leader in the analytical instrument industry for nearly 50 years, Beckman is credited with creating the most recent "Beckman DU series 60 spectrophotometer, it uses two distinct light sources, either an H2 or D2 lamp, to measure in the visible range, allowing measurements between 190 and 1000 nm. Electromagnetic radiation interaction with matter is studied in UV-VIS spectroscopy. Matter either absorbs or emits energy in discrete amounts known as quanta [14]. It is employed in the analysis of various solvent types and materials, including inorganic, organic, and biomolecules, and is primarily favored for its ease of maintenance, simplicity, adaptability, speed, and cost-effectiveness. It is employed in the identification, quantification, evaluation, and purification of many substances [15]. It is a measurement tool that is typically used for quantitative analysis of chemical substances. It works by figuring out how much light is partially absorbed by the analyte in the solution [2]. It can be categorized by spectral region, which includes near infrared (from 800nm to 2500nm), VIS (from 380nm to 750nm), and UV (from 190nm to 380nm) [16]. The fundamental idea is that the excitation of electrons from low to high energy levels is connected to the absorption of visible and UV light (200–400 nm) [17]. It is also referred to as electron spectroscopy and entails the observation of electrons [18]. It includes measuring the amount of electromagnetic radiation (EMR) that a sample's molecules, atoms, or ions release or absorb when they change from one energy state to another. The transition could occur from the ground state to the excited state or vice versa [2]. This physical method makes use of light in the visible, ultraviolet, and near-infrared spectrums [3]. UV-VIS Spectroscopy was employed in clinical laboratories for a long time. Over time, there has been less and less reliance on UV light. For a long time, clinical laboratories used UV-VIS spectroscopy. There has been a decreasing need on UV light throughout time [19]. An region called a chromophore is where electronic changes happen. Radiation can absorb a certain quantity of radiation when it passes through a transparent substance. When residual radiation is passed through a prism, if it occurs, the resultant spectrum is called an absorption spectrum because it has gaps in it. From the ground state, which is the lowest energy level, to the excited state, which is the highest energy state, the atoms (or) molecules migrate [20].

have been created to measure the ions of heavy metals. UV-visible spectrophotometry is one of these methods that is most frequently employed because of its benefits in terms of speed, accuracy, ease of use, cost-effectiveness, and adaptability [21]. Without the need for any separation processes, ultraviolet-visible spectrophotometry is a commonly used traditional quantitative detection technique that may be used to estimate the concentration of metals in a solution [22].

In this research review, I utilized ultraviolet-visible (UV-Vis) spectroscopy to determine the concentrations of metal ions in a solution containing multiple metals. I focused on three specific ions: Cu^{2+}, Pb^{2+}, and Cd^{2+}.

2. Principle

UV/Visible Spectroscopy is the study of a sample's light reactivity. A monochromatic light beam may absorb a certain percentage of light as it passes through the sample, with the remaining light being transmitted through it [23]. It is a method based on measuring how much electromagnetic radiation is absorbed by a material. Electromagnetic radiation depletion can be caused by

interference, absorption, scattering, or reflection. This radiation's spectral range is about between 190 and 800 nm [24]. Chemical compounds absorb ultraviolet or visible light to produce a specific spectrum. The interaction of light and matter is the fundamental concept of spectroscopy. When a substance absorbs light, activation and de-excitation can happen, which can result in the formation of a spectrum. When an electromagnetic wave hits a substance, it can cause a variety of effects, including transmission, absorption, reflection, and scattering. The electronic transition principle explains how a particle is excited from the state of grounding to its state of excitation and is involved in ultraviolet-visible spectroscopy [25]. The sample may absorb light in the visible or ultraviolet spectrum when monochromatic light travels through it. Through the absorption of light, electrons are stimulated from a smaller energy orbit (the highest occupancy molecule orbital (HOMO) to a more energetic empty orbiting (the lower unfilled molecular orbital (LUMO) [26, 27]. Bandgap energy (ΔE) for the HOMO-LUMO energy gap must be equal to the power of the absorbed light wavelength (Figure1) [28, 29].

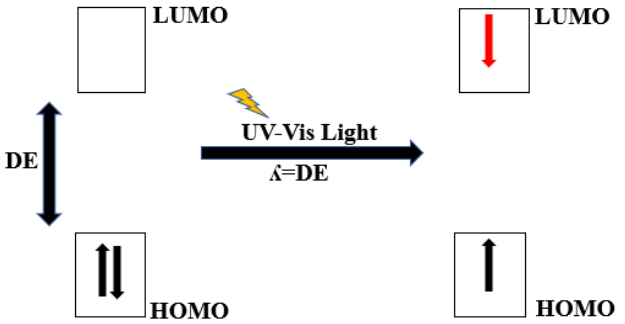

Figure (1): The electron energy state can be excited by molecular orbitals and the required energy gap

Three kinds of lower energy ground state orbitals could be relevant: σ molecular orbital (bonding), π Molecular orbital (bonding) and n atomic orbital (nonbonding). Two different kinds of anti-bonding orbitals could be at play: π^* $(pi-star)$ and σ^* $(sigma-star)$ orbital.
As n electrons do not establish bonds, there is no n^* orbital anti-bonding. The following are the electronic transitions brought about by visible and ultraviolet light absorption. This brief statement introduces the absence of n^*anti-bonding orbitals due to non-bonding n electrons and previews the subsequent discussion on electronic transitions induced by visible and ultraviolet light absorption. (σ to σ^*) and (π to π^*) and (n to σ^*) and (n to π^*) Transition. High energy is needed for the σ to σ^* and n to σ^*transitions, which occur in the 180 nm–240 nm range or in the far ultraviolet region [2].

2.1. Components of UV-visible spectroscopy

The following parts make up instruments used to measure the absorption of UV or visible radiation: (Source. Monochromator. Sample cell. Detector. Readout system a. Amplifier b. Display).

2.1.1. Source of light

UV radiation sources: The radiation source's power mustn't fluctuate significantly across its wavelength range. A continuous UV spectrum is produced when deuterium or hydrogen are electrically excited at low pressure. The creation of an excited molecular species causes this, which splits into an ultraviolet photon and two atomic species. This can be displayed as:

$$\text{electrical energy} + D2 \rightarrow D2* \rightarrow D' + D'' + hv$$

The wavelength range for radiation emitted by deuterium (D) and hydrogen lamps is 160–375 nm. These lamps must employ quartz windows. Because glass absorbs radiation with wavelengths less than 350 nm, quartz cuvettes must be utilized [4]. Visible radiation sources: Visible light is frequently produced using tungsten filament lamps. The wavelength range for this kind of light is 350–2500 nm. A tungsten filament lamp's energy output is proportional to the voltage at which it operates, raised to the fourth power. This implies that the voltage to the lamp needs to be extremely stable in order for the energy output to be stable. This stability is ensured by constant-voltage transformers or electronic voltage regulators [30].

Figure (2): The Light source Deuterium lamp is used UV radiation

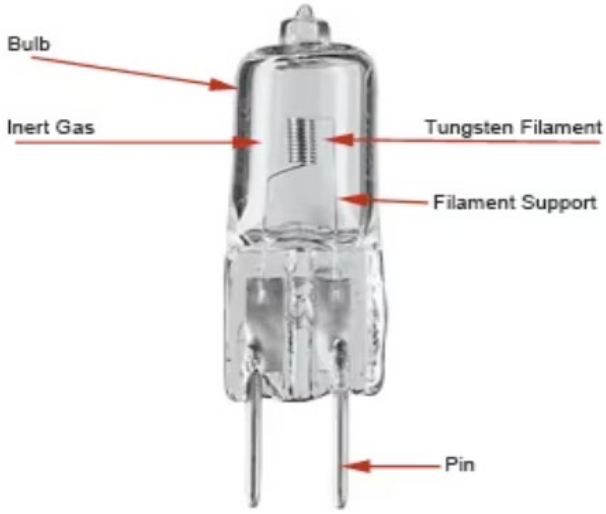

Figure (3): The Light source Tungsten halogen lamp is used visible radiation

2.1.2. The Monochromator (Wavelength selector)

Light is divided into its constituent wavelengths by a monochromator, which then chooses a small range of wavelengths to send to the sample or detector. A wavelength selector should ideally produce radiation with a single wavelength as its output. A band of radiation is often obtained; a genuine wavelength selection is not optimum. They are employed in spectrum scanning, which is the process of changing the radiation's wavelength over a wide range. They are applicable to the UV/Vis area. Mechanically, all monochromators are made similarly. Lenses, gratings, prisms, slits, mirrors, and lenses are all used in monochromators [31].

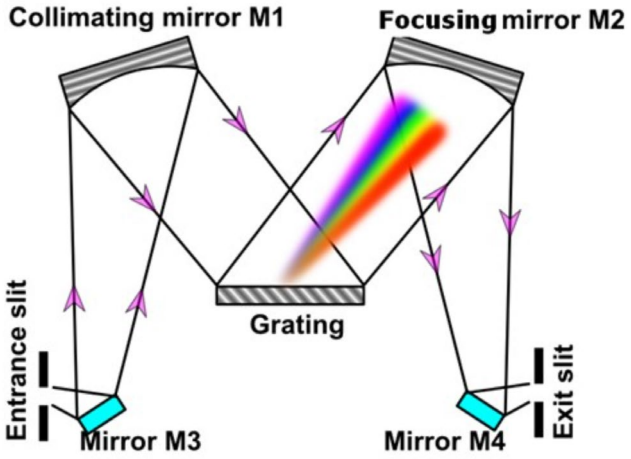

Figure (4): Turner grating Monochromator

2.1.3. Sample cell

The radiation that will pass through the sample and reference solution containers must be visible through them. For UV spectroscopy, quartz or fused silica cuvettes are needed. These cells are also transparent in the visible spectrum. Cuvettes for use in the 350–2000 nm range can be made from silicate glasses. This succinct description outlines the requirements for cuvettes in UV spectroscopy and their compatibility with different materials across the UV and visible spectra [32].

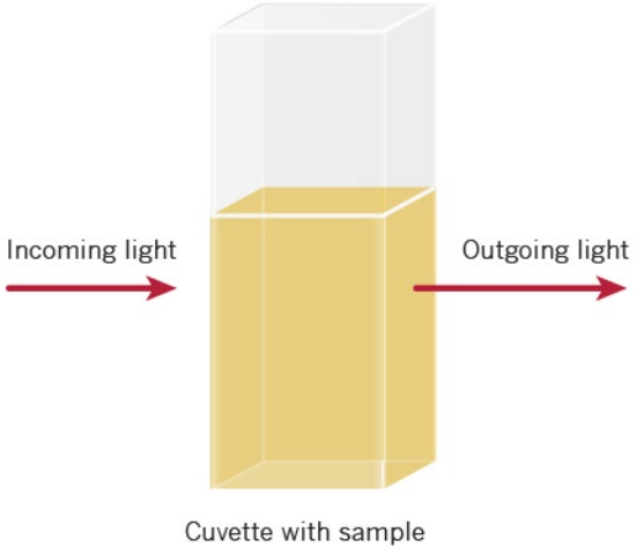

Figure (5): Cuvette with sample

2.1.4. Detector

The detectors are apparatuses that translate light from the sun into electrical signals. A detector needs to be fast-responding and sensitive across a wide range of wavelengths. Furthermore, the detector's electrical signal needs to have a linear response, meaning it should be directly proportionate to the transmitted intensity [15]. Two types of detectors: When exposed to visible or ultraviolet light, a photosensitive, negatively charged cathode releases electrons. Electrons traverse a vacuum to reach an anode, where they generate a current that is directly proportional to the intensity of radiation. This brief statement captures the essential process wherein electrons, traveling through a vacuum, contribute to the generation of current, and this current is directly correlated with the intensity of the incident radiation. Electrons from the photosensitive cathode impact a second surface, known as the dynode, which is positive in relation to the original cathode in this extremely sensitive gadget. As a result, electrons accelerate and can remove multiple electrons from the dynode. For every photon striking the initial cathode, more than 10^6 electrons are eventually gathered if the procedure above is performed multiple times. This statement underscores the substantial amplification achieved through the described process, emphasizing the significant increase in the number of electrons collected from each photon.

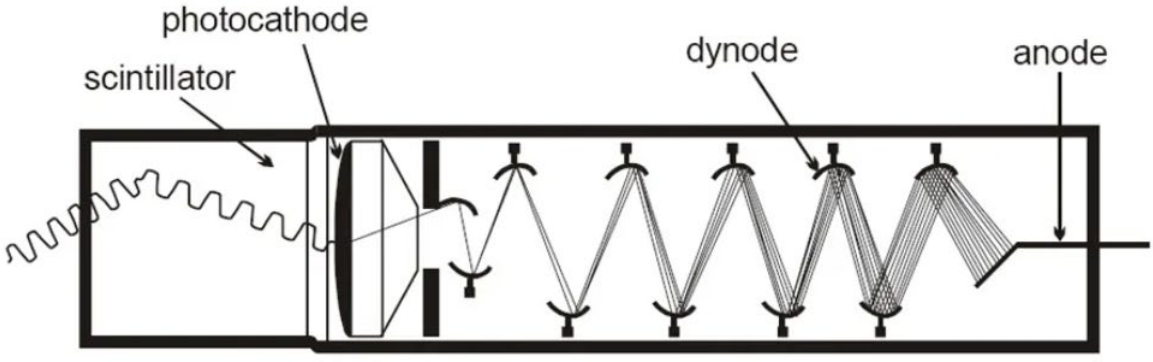

Figure (6): The Photomultiplier tube detector

3. Instrument Designs for Molecular UV/Vis Absorption

The filter photometer, now the most basic equipment for molecular UV/V is absorption, isolates a band of radiation using an absorption or interference filter. The filter shields the sample from high-energy radiation. This concise description underscores the essential role of a filter photometer in isolating specific radiation bands for molecular absorption analysis in the UV/V is range. A filter photometer, often known as a singular-beam apparatus, consists of just one optically route connecting the source and detector. The shutter is employed to prevent the source radiation from the detector when the apparatus is set up to 0% T. [15, 33]. After the shutter has been removed, the device is set up to 100% transmittance (T) employing a suitable blank. After reintroducing the blank and sample, the transmittance is measured. Calibration is required every time the filter is replaced, as both the incident power from the source and the detector's sensitivity fluctuate with wavelength. This brief statement highlights the calibration process and the need for recalibration when changing the filter in the photometer [4]. Photometers have an advantage over other spectroscopic instruments in that they are easy to maintain, robust, and reasonably priced. A photometer's portability is another benefit that makes it an effective tool for doing spectroscopic analyses in the field. A photometer's inability to produce an absorption spectrum is one of its drawbacks [34]. Figure (3) instrumentation UV-visible spectroscopy:

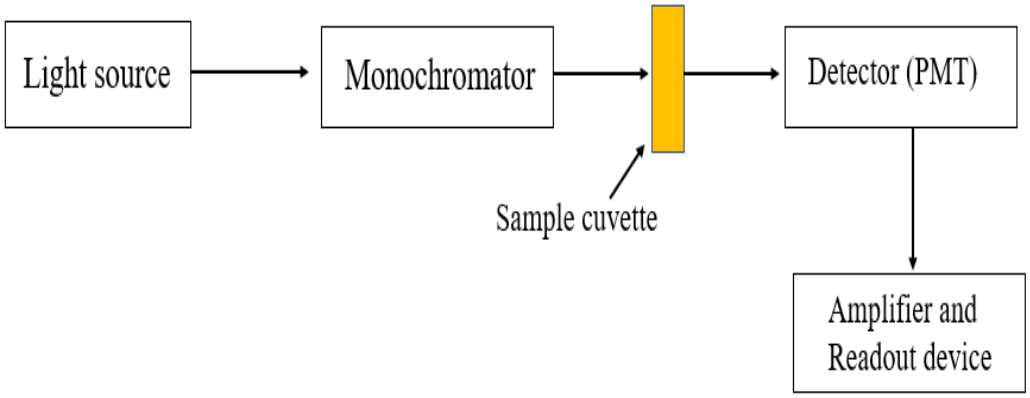

Figure (7): Instrumentation UV-visible spectroscopy single beam

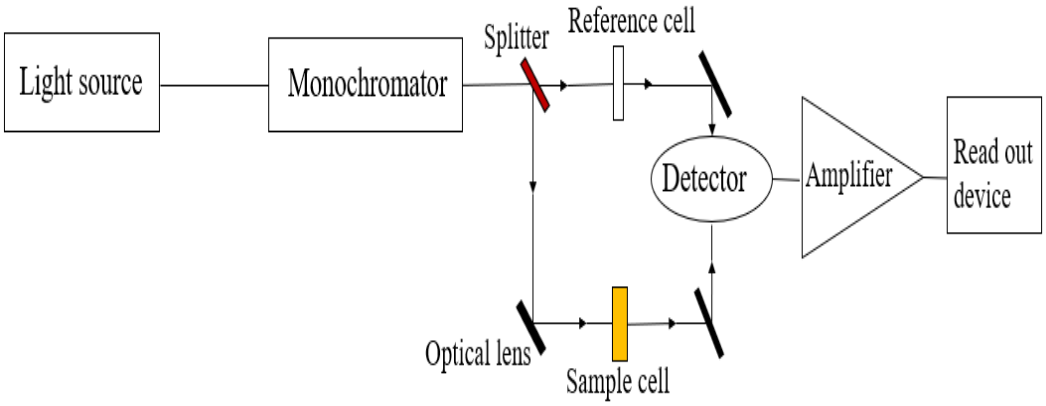

Figure (8): Instrumentation UV-visible spectroscopy double beam

4.

5. Applications of Characterization

Chemical absorbing has been widely used in a wide range of characterization studies, especially for the UV/V is band. It has been useful in establishing constants of equilibrium and figuring out the ratios of metal-ligand compounds. The experiments' use of molecular absorption illustrates its adaptability as a useful analytical tool that offers insightful information on the characteristics and nature of chemical substances, particularly those involving metal-ligand reactions [34].

5.1. Stoichiometry of a Metal–Ligand Complex

A general type of reaction includes the stoichiometry of the metal-ligand association processes, which is a critical factor in determining the number of ligands binding with transition metals (M), by the ligand-transition (L) metal interaction represented by this equation:

$$M + L_y \leftrightarrow M(L)_y$$

5.2. Determination of Equilibrium Constants

Another significant use of molecule absorption is the identification of equilibrium constants. As a basic example, let's look at an acid-base reaction in general. This application demonstrates the value of molecular absorption in quantifying the size of chemical reactions by providing important information about the equilibrium state and the balance between reactants and products in a range of chemical processes.

$$HIn + H_2O \leftrightarrow H_3O + In^-$$

An indicator's HIn and In- in-equilibrium is vital, revealing sensitivity to acidity or basicity changes. In order to efficiently display pH changes during chemical interactions or titrations utilizing acid-base indicators:

$$\mathrm{Ka} = [\mathrm{H_3O+}][\mathrm{In-}]/[\mathrm{HIn}]$$

Establishing an equilibrium state for the process and measuring the equilibrium concentrations (Ka) of H3O+, HIn, and In- allow us to determine the value of the equilibrium constant [34].

6. Determinations Metal Ion

Beer's and Lambert's laws are briefly summarized in the Beer-Lambert–Bouguer equation, a fundamental guide for absorbance measurement in analytical spectroscopy. This sentence shows how the absorbance varies in the spectral region where Beer's law applies:

$$A = abc$$

To the Beer-Lambert equation, a long wavelength at which light greatly affects both absorbance and absorptivity, where A is the absorbance b is the pass length, c is the analytes concentrated, and a is the absorptivity. This correlation illustrates the wavelength-dependent nature of absorption properties in analytical spectroscopy [35]. When concentration is represented using molarity, absorptivity is substituted with molar absorptivity, ε (with units of cm^{-1} M-1). Both absorptivity and molecular absorptivity essentially show how likely it is that an analyte is to absorb one photon of a particular energy. These parameters serve as crucial measures in determining the propensity of analyte absorption at specific energy levels, providing essential insights into the analytical characteristics of the substance [34].

To determine the amount of metal ions or cons of analyte, I employ a calibration curve. This curve is constructed by plotting the absorbance against analyte concentration in a series of standard solutions. According to Beer's rule, the calibration curve ought to be a single line with a slope denoted by (ab), and a point of intersection of (0). This linear relationship allows for accurate quantification of analyte concentration in unknown samples based on their absorbance values [36]. Figure (2).

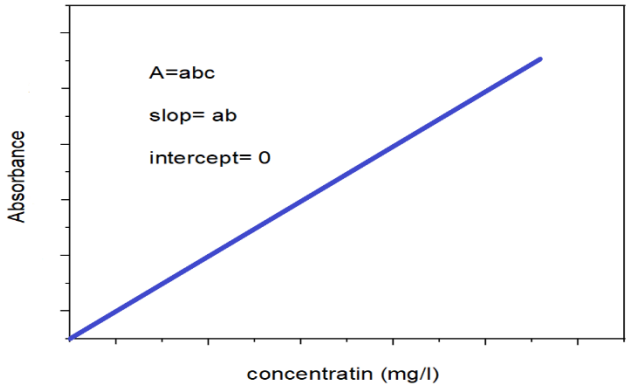

Figure (9): Quantitative analysis using a standard curve.

The three metal ions—Copper (II), Cd^{2+}, and Pb^{2+}—have individual maximum absorption wavelengths (λ-max) of 755 nm, 323.9 nm, and 10-380 nm, respectively. However, when they interact with different reagents, the maximum absorption wavelength (λ-max) for each ion changes. As shown in Table 1 below, compiled from various sources, the λ-max values of Cu^{2+}, Pb^{2+}, and Cd^{2+} are determined using different reagents.

Table (1): λ-max the three metallic ions (Cu^{+2}, Pb^{+2}, and Cd^{+2}) by different reagent

No.	Metal ion	Reagent	$\lambda_{\text{-max}}$	Ref.
1	Copper (II)	immobilized ligand	550 nm	[37]
2	Copper (II)	2- amino derivative-1,2,3-thiadiazole	525 nm	[38]
3	Copper (II)	malachite ($Cu_2CO_3(OH)_2$	821 nm	[39]
4	Copper (II)	4-methyl-2-((quinolinyl-8-amino) methyl) phenol	855 nm	[40]
5	Copper (II)	2,7-bis(*o*-arsenophenyl)azo	520 nm	[41]
6	Copper (II)	basic medium to form a Cu–metformin complex. The complex is dissolved in cyclohexylamine	540 nm	[42]
7	Copper (II)	thiosemicarbazide as complexing agent	356 nm	[43]
8	Copper (II)	chromogenic reagent di-2-pyridyl ketone benzoylhydrazone (dPKBH) in an alkaline medium	370 nm	[44]
9	Copper (II)	2,3,4,6/-Tetrahydroxy-3/-Sulfoazobenzene in Real Samples	485 nm	[45]
10	Copper (II)	Michler's thioketone Reagent	646 nm	[46]
11	Copper (II)	piperazine as ligand in ammonium acetate medium	560 nm	[47]
12	Copper (II)	2-hydroxyphenones	300-800 nm	[48]

13	Copper (II)	$Cu(3,5\text{-}Cl)_2$	750 nm	[49]
14	Copper (II)	1,8 dihydroxynaphthalene	620 nm	[50]
15	Copper (II)	$Cu(5\text{-}Br)_2$	720 nm	[49]
16	Copper (II)	$Cu(4,5\text{-}Cl)_2$	723 nm	[49]
17	Copper (II)	$Cu(5\text{-}Cl)_2$	707 nm	[49]
18	Copper (II)	3,6-disulfonic acid (arsenazo III)	540 nm	[50]
19	Copper (II)	$Cu(HBP)_2$	674 nm	[49]
20	Copper (II)	$Cu(4\text{-allyloxy})_2$	660 nm	[49]
21	Copper (II)	5-diethylaminophenol	520 nm	[51]
22	Copper (II)	$Cu(4\text{-}OMe)_2$	658 nm	[49]
23	Copper (II)	$Cu(HAP)_2$	655 nm	[49]
24	Copper (II)	$Cu(HPP)_2$	650 nm	[49]
25	Lead (II)	tris(2-quinolylmethyl)amine	480 nm	[52]
26	Lead (II)	1-(2-pyridylazo)-2-naphthol reacts in slightly acidic solution	548 nm	[53]
27	Lead (II)	Hydride generation	283.3 nm	[54]
28	Lead (II)	1,5-diphenylthiocarbazone in aqueous micellar	500 nm	[55]
29	Lead (II)	5-diethylaminophenol	520 nm	[51]
30	Lead (II)	diphenylthiocarbazone complex on an Amberlite XAD-1180 column	486 nm	[56]
31	Lead (II)	2-(5-bromo-2-pyridylazo)-5-dimethylaminophenol in ethanolic medium has been developed	455 nm	[57]
32	Lead (II)	cyanidin (3, 3-4,5,7-pentahydroxyflavylium chloride)	389.6	[58]
33	Lead (II)	8-hydroxyquinoline,7-(6-methoxy2-benzothiazolyl azo)	524 nm	[59]
34	Lead (II)	using murexide reagent in mixed solvent system	504 nm	[60]
35	Lead (II)	3,6-disulfonic acid (arsenazo III)	520 nm	[41]
36	Lead (II)	dithiazone	500 nm	[61]
37	Lead (II)	diethyldithio-carbamate	435 nm	[62]
38	Lead (II)	4-(2-pyridilazo) resorcinol	520 nm	[63]
39	Lead (II)	diphenylcarbazone	**545 nm**	[64]
40	Lead (II)	2,7-bis(*o*-arsenophenyl)azo	**520 nm**	[41]
41	Lead (II)	Arsenazo (III)	538 nm	[65]
42	Lead (II)	2-(2-thiazolylazo)-*p*-cresol	588 nm	[66]
43	Lead (II)	1,8 dihydroxynaphthalene	520 nm	[50]
44	Lead (II)	porphyrin compounds	410 nm	[67]
45	Cadmium (II)	4-(2-thiazolylazo) resorcinol	492 nm	[68]
46	Cadmium (II)	5,7-dibromo-8-hydroxyquinoline (DBHQ) has been developed	396 nm	[69]
47	Cadmium (II)	2-hydroxy-4-n-butoxy-5-bromopropiophenone thiosemicarbazone	440 nm	[70]
48	Cadmium (II)	4-(2-pyridylazo)-resorcinol	510 nm	[71]
49	Cadmium (II)	Diacetylmonoxime-3-amino-4-hydroxy benzoyl hydrazone (DMAHBH)	378 nm	[72]
50	Cadmium (II)	2-amino-cyclopentene-1-dithiocarboxylic acid	430 nm	[73]
51	Cadmium (II)	"[4-((imidazole-2-yl)diazenyl)-N-(pyrimidin-2-yl)benzenesulfonamide]" (IDPBS) at basic media	441 nm	[74]
52	Cadmium (II)	Ammonium pyrrolidinedithiocarbamate (APDC)	452 nm	[75]
53	Cadmium (II)	cyanidin (3, 3-4,5,7-pentahydroxyflavylium chloride)	357.8 nm	[58]
54	Cadmium (II)	8-hydroxyquinoline,7-(6-methoxy2-benzothiazolyl azo)	550 nm	[59]
55	Cadmium (II)	sulphide/poly(vinyl alcohol) nanocomposite films	515 nm	[76]

56	Cadmium (II)	[4-((imidazole-2-yl)diazenyl)-N-(pyrimidin-2-yl)benzenesulfonamide]"	441 nm	[74]
57	Cadmium (II)	using murexide reagent in mixed solvent system	483 nm	[60]
58	Cadmium (II)	1- propanone-1-(3chlorophenyl) - 2-[(1,1dimethylethyl) amino] hydrochloride	252 nm	[77]
59	Cadmium (II)	2-(5-bromo-2-pyridylazo)-5-diethyl aminophenol	530 nm	[78]
60	Cadmium (II)	1,10-phenanthroline	400 nm	[79]
61	Cadmium (II)	2-(5-bromo-2-pyridylazo)-5-(diethylamino)phenol	550 nm	[68]
62	Cadmium (II)	2-hydroxy-4-n-butoxy-5-bromopropiophenone thiosemicarbazone	440 nm	[70]
63	Cadmium (II)	1-(2-pyridylazo)-2-naphthol	420 nm	[80]
64	Cadmium (II)	2,7-bis(*o*-arsenophenyl)azo	520 nm	[41]
65	Cadmium (II)	1,8 dihydroxynaphthalene	520 nm	[50]
66	Cadmium (II)	3,6-disulfonic acid (arsenazo III)	520 nm	[41]
67	Cadmium (II)	5-diethylaminophenol	520 nm	[51]

As explained in this figure (6), the spectrum of each of the metal ions (Cu^{+2}, Pb^{+2}), by Ultraviolet-visible spectrophotometer is shown.

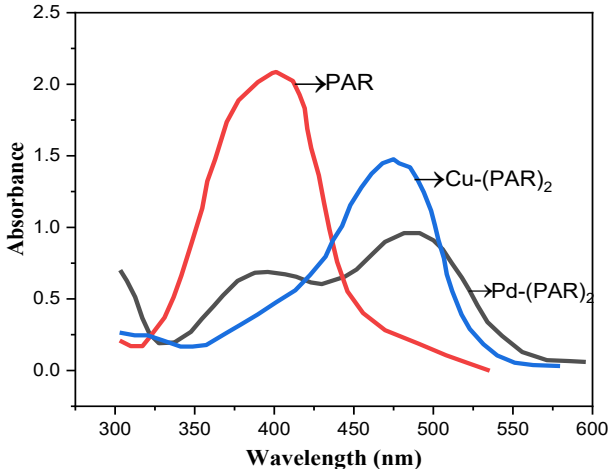

Figure (10): The PAR, Pb (PAR) 2, and Cu-(PAR) 2 complexes' UV-Vis spectrum

7. Evaluation

The most significant aspect of UV-visible spectroscopy for metal ion determination lies in the meticulous evaluation of absorption peaks, establishing correlations with known metal ion properties to quantify their concentration in the analyzed sample precisely. The method for measuring light absorption in the ultraviolet and visible regions of the electromagnetic spectrum is termed UV-visible spectroscopy. This technique is employed to ascertain the presence of metal ions, involving the identification of the wavelength at which a particular metal absorbs light [81].

7.1. Scale operation

Molecular UV/Vis absorption is a commonly employed method for analyzing trace analytes in both large (macro) and medium-sized (meso) samples. UV-visible spectroscopy stands out as a powerful tool for the analysis of trace analytes in various sample sizes. It excels in determining major and minor analytes, offering the flexibility to handle ultra-trace analytes through methods such as dilution or concentration. In contrast, the operational efficiency of infrared absorption is commonly perceived to be inferior to that of UV/Vis absorption.

7.2. Accuracy

Under normal conditions, UV/Vis absorption readily yields relative errors of 1-5 percent. In most cases, accuracy is influenced by the blank's quality. The existence of particles in a sample that scatter radiation and interference that reacts with analytical reagents are two examples of the kinds of issues that could arise.

7.3. The precision

When measuring absorbance, undetermined errors, or instrumental "noise," are introduced that restrict the precision of absorption spectroscopy. Because it can be difficult to discern even a tiny difference between P_0 and P_T, precision is typically worse at extremely low absorbances and very high absorbances when P_T is close to 0. Therefore, we might anticipate that precision will change when transmittance changes. To address these challenges, researchers often employ statistical approaches, calibration procedures, and optimized experimental conditions to enhance precision across a wide range of absorbance values. Continuous refinement of methodologies and instrumentation contributes to advancing the precision capabilities of UV/Vis absorption measurements. Managing and understanding these factors are critical for ensuring reliable and accurate absorption spectroscopy results across a range of absorbance values.

7.4. Selectivity

Selectivity is seldom an issue In the field of molecule absorption spectroscopy. Often, Finding a wavelength at which the analyte alone absorbs is possible, or applying chemical processes to guarantee that the analyte was the only species absorbing during the chosen wavelength. This capability to achieve high selectivity enhances the specificity of molecular absorption spectrophotometry,

allowing for precise and accurate measurements with minimal interference from other substances in the sample.

7.5. Equipment, Time, and Cost

Using an absorption spectrophotometer for analyzing a sample is generally a swift process, although additional time may be necessary in cases where a To change a nonadsorbing substance to an absorption form, a reaction chemical is required. UV/Vis equipment varies greatly in price, starting at several thousand dollars for a simple, manually controlled, one-beam device with a less expensive grating compared to an expensive, excellent quality, double-beam device with movable slits that can function in a wider wavelength range. The investment in instrumentation often aligns with the complexity and features required for specific analytical needs [82].

8. Application

UV-vis spectroscopy has a wide range of uses: Quantitative analysis, Molecular weight determination, and Quantitative analysis of pharmaceutical substances, Structural elucidation of organic compounds, Detection of impurities, and qualitative analysis. Chemical analysis, Dissociation constant of acids and bases, As HPLC detector [15, 83]. In raw ores, mineral wastes, and wastewater, iron typically coexists with non-ferrous metals [84, 85]. Human health is fatally affected by high environmental iron exposure levels [86]. Excessive Fe2+ and Fe3+ in the biometallurgical and hydrometallurgical processes will negatively impact the quality of the metal products and seriously impair the electrolysis process that follows [87]. Determining the iron concentration in hydrometallurgical and environmental samples fast and reliably is therefore crucial. One important method for smelting zinc is hydrometallurgy. Hydrometallurgy's industrial effluent typically contains a large number of overproof trace metal ions, whose concentrations must be carefully regulated and determined in real-time. Currently, a number of techniques, including voltage measurement, the analysis of atomic absorption (AAS), and ultraviolet-visible spectroscopy have been proposed for the simultaneous detection of metal ions [88-90]. After many years of widespread use, ultraviolet-visible (UV-Vis) spectroscopy has grown to be a highly important analytical technique in contemporary labs. Although there are numerous areas where alternative methods can be employed, UV-Vis spectroscopy is preferable due to its adaptability, ease of use, accuracy, speed, and affordability [89, 91]. UV-Vis's spectroscopy is a commonly used quantitative analysis technique for figuring out the concentration of metals in metal complexes in solution. Analysts are becoming more and more interested in simultaneously determining many metals in order to eliminate the separation stage.

Figure (7) displays the absorption spectra in the (350 nm–800 nm) wavelength range for copper, cobalt, nickel, and their mixture. Ratio derivative spectrophotometry is a highly helpful tool in both the quantitative and qualitative examination when determining multicomponent mixes using a zero-crossing approach when combined overlap and interference exists. Nevertheless, a significant drawback is that noise is increased when calculating derivatives, resulting in a decrease in ratio of signals to noisy (the SNR). This work proposes a novel technique for the concurrent measurement of ternary combinations of nickel, cobalt, and copper using UV-Vis spectroscopy, without the need for a separation phase. The technique combines ratio spectrum derivation with continuously the wavelet transformation [92].

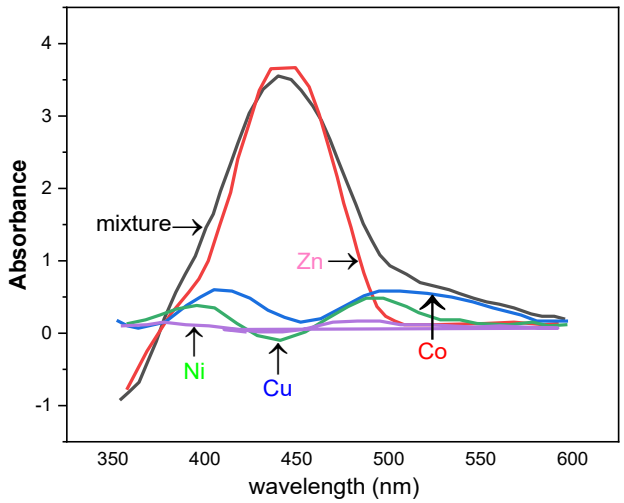

Figure (11). The absorbance spectrum of 2.4 mg/L of copper (Cu), 1.2 mg/L of cobalt (Co), 1.8 mg/L of nickel (Ni), and their combination.

Based on the production of the copper-Chloro-(phenyl) glyoxime complex, a straightforward approach for the spectrophotometric detection of trace quantities of copper is described. At 290.5 nm and pH 4.0, the complexes' molar absorptivity were 0.8 × 104 l/mole cm. The ideal reagent quantities and pH levels have been determined for copper determination [93]. Additionally, the impacts of the foreign ions were examined. The technique was effectively used to measure the amount of copper present in various natural fluids and pharmaceutical samples. Copper is also a regularly found element in natural waterways. The majority of drinking water copper pollution happens in the water distribution system due to copper tubing or fittings corroding. The identification of heavy metal ions in their inorganic or organic complexes can still be accomplished with the use of ultraviolet-visible spectrophotometry, an instrumental technique. Numerous spectrophotometric techniques have been put forth to determine the copper concentration in a range of materials, including pharmaceutical and natural water samples [94].

Ions of (Pb^{2+}) and (Cu^{2+}) are prevalent contaminants found in water that could potentially be extremely harmful to people's health. This work the purpose of its assessment of concentrations of lead and copper ions in aqueous solution without wasting chemical reagents by direct UV detection. Lead and copper ions are measured using UV wavelengths ranging from 205 to 225 nm, with a detection range of 0.2 mg/L to 10 mg/L. The method was effectively used on a high-performing synthetic sample [95].

Nevertheless, the majority of conventional spectrophotometric systems are not suitable for identifying samples with robust ligands and complicated matrices. Nevertheless, the majority of conventional spectrophotometric systems are not suitable for identifying

samples with robust ligands and complicated matrices. For the purpose of determining trace iron, current UV-Vis procedures do not follow Beer-Lambert's law because of the test system's low sensitivity and selectivity. Fe^{2+} and Fe^{3+} concentrations in aqueous samples are often measured independently, or Fe2+ should be subtracted after Fe3+ has been oxidized to calculate total iron. These techniques compensate for the low sensitivity and chemical interferences that can occur while determining iron in watery samples. Unfortunately, the lengthy and intricate sample pretreatment process is unable to satisfy the demands of quick analysis in industrial online applications. Due mostly to the differing UV–vis absorption characteristics of Fe^{2+} and Fe^{3+}, there is currently no way to determine the mixed solution system including Fe^{2+} and Fe^{3+} directly without separation or preconcentration [93].

The keywords in this research review are (Ultraviolet-visible spectroscopy, Metal ion, Beer's, and Lambert's Law), which has seen a complete improvement from 1990 to 2022, as shown in this (Figure 7) Science Network Resource. The increasing trend observed in the columnar lines over time emphasizes the importance of reviewing this paper which includes (Ultraviolet-visible spectroscopy, metal ion, Beers and Lamberts law), This pattern indicates the growing importance of these topics, suggesting their widespread use across different walks of life.

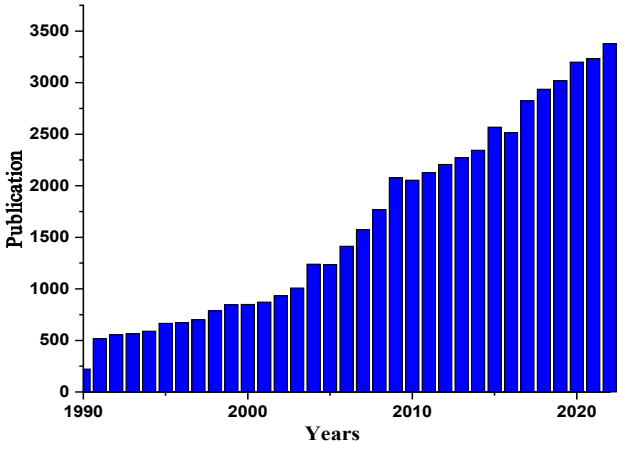

Figure (12): Growth of my keywords in my research review the source of web Science.

9. Conclusion

Metal ion analysis is made possible by ultraviolet (UV) spectroscopy, which measures the amount of UV light that metal complexes absorb. I have detected three separate maximum absorption wavelengths (λ-max) for metal ions (Cu^{2+}, Pb^{2+}, and Cd^{2+}) that change in response to different reagents. This technique is useful for comprehending the electrical structures of metal complexes and how they develop in solutions. Recognizing distinctive absorption bands, connecting them to particular metal ions, and utilizing calibration curves for precise quantification are important factors to take into account. This method provides an easy-to-use method for measuring numerous ions at once and is particularly helpful in figuring out copper concentrations in natural water sources and pharmaceutical samples. Pb^{2+}, Cd^{2+}, and Cu^{2+} are among the metal ions that have been researched in aquatic systems for possible applications in metal detection and separation procedures, especially for environmentally important metals. In analytical chemistry, UV/VIS spectroscopy is an effective instrument that is frequently utilized to measure analytes such as conjugated compounds, transition metal ions, and biological macromolecules.

References:

1. G.D. Christian, P.K. Dasgupta, and K.A. Schug, *Analytical chemistry*. 2013: John Wiley & Sons.
2. N. Sudharshan and V. Swetha, UV-VISIBLE SPECTROSCOPY: A COMPREHENSIVE REVIEW ON INSTRUMENTATION. 2023.
3. S.J.I.J.o.P.R. Vijayraj and Analysis, Analytical process of drug by ultraviolet (UV) spectroscopy: A review. 2012. **2**(2): p. 72-78.
4. D.A. Skoog, F.J. Holler, and S.R. Crouch, *Instrumental analysis*. Vol. 47. 2007: Brooks/Cole, Cengage Learning Belmont.
5. K.N. Aziz, et al., A review of coordination compounds: structure, stability, and biological significance. *Reviews in Inorganic Chemistry*, 2024(0).
6. B. Bansod, et al., A review on various electrochemical techniques for heavy metal ions detection with different sensing platforms. 2017. **94**: p. 443-455.
7. K.N. Aziz, et al., Organometallic complexes and reaction methods for synthesis: a review. *Reviews in Inorganic Chemistry*, 2024(0).
8. R.A. OMER, et al., Computational and spectroscopy study of melatonin. *Indian Journal of Chemistry-Section B (IJC-B)*, 2021. **60**(5): p. 732-741.
9. H. Ismail, et al., Synthesis, Characterization, and Computational Insights Into the Conductive Poly (p-aminophenol). *Russian Journal of Physical Chemistry B*, 2024. **18**(4): p. 1148-1165.
10. L. Sommer, *Analytical absorption spectrophotometry in the visible and ultraviolet: the principles*. 2012: Elsevier.
11. B.M. Weckhuysen, P. Voort, and G. Catana, *Spectroscopy of transition metal ions on surfaces*. 2000: Leuven University Press.
12. A. Vogler and H. Kunkely, Photoreactivity of metal-to-ligand charge transfer excited states. *Coordination chemistry reviews*, 1998. **177**(1): p. 81-96.
13. C.P. Bacon, Y. Mattley, and R.J.R.o.S.i. DeFrece, Miniature spectroscopic instrumentation: Applications to biology and chemistry. 2004. **75**(1): p. 1-16.
14. D.M.K. Panchal, et al., A REVIEW ON "HIGH PERFORMANCE THIN LAYER CHROMATOGRAPHY". 2022.
15. G. Verma and M.J.W.J.P.R. Mishra, Development and optimization of UV-Vis spectroscopy-a review. 2018. **7**(11): p. 1170-1180.
16. D. González-Morales, et al., Development of a low-cost UV-Vis spectrophotometer and its application for the detection of mercuric ions assisted by chemosensors. 2020. **20**(3): p. 906.
17. D.M. Atole and H.H.J.A.J.p.c.r. Rajput, Ultraviolet spectroscopy and its pharmaceutical applications-a brief review. 2018. **11**(2): p. 59-66.

18. I.I. Mut Günzler and A.J.E. Williams, Handbook of analytical techniques,. 2001. **1**: p. 1.2.
19. S.L.J.E.o.a.c. Upstone, Ultraviolet/visible light absorption spectrophotometry in clinical chemistry. 2000: p. 1699-1714.
20. D.L. Pavia, et al., *Introduction to spectroscopy*. 2014: Cengage learning.
21. W. Cheng, et al., Direct-determination of high-concentration sulfate by serial differential spectrophotometry with multiple optical pathlengths. 2022. **811**: p. 152121.
22. F. Zhou, et al., A spectrophotometric method for simultaneous determination of trace ions of copper, cobalt, and nickel in the zinc sulfate solution by ultraviolet-visible spectrometry. 2019. **223**: p. 117370.
23. L.H. Abdel-Rahman, et al., Synthesis, characterization, biological and docking studies of ZrO (II), VO (II) and Zn (II) complexes of a halogenated tetra-dentate Schiff base. 2022. **15**(5): p. 103737.
24. M.L. Passos and M.L.M.J.M. Saraiva, Detection in UV-visible spectrophotometry: Detectors, detection systems, and detection strategies. 2019. **135**: p. 896-904.
25. F.S. Rocha, et al., Experimental methods in chemical engineering: Ultraviolet visible spectroscopy—UV-Vis. 2018. **96**(12): p. 2512-2517.
26. R.A. Omer, et al., Combined DFT and Monte Carlo simulation studies of potential corrosion inhibition properties of coumarin derivatives. *Journal of Molecular Modeling*, 2024. **30**(8): p. 288.
27. Y.H. Azeez, et al., Combined DFT and Monte Carlo simulation studies of potential corrosion inhibition properties of heterocyclic derivatives with an extended π-System. *Computational and Theoretical Chemistry*, 2024. **1240**: p. 114803.
28. M. Sauer, J. Hofkens, and J. Enderlein, *Handbook of fluorescence spectroscopy and imaging: from ensemble to single molecules*. 2010: John Wiley & Sons.
29. Y.H. Azeez, et al., Investigation of corrosion inhibition and adsorption properties of quinoxaline derivatives on metal surfaces through DFT and Monte Carlo simulations. *Corrosion Reviews*, 2024(0).
30. Y.R. Sharma, *Elementary organic spectroscopy*. 2007: S. Chand Publishing.
31. G. Shinde, et al., A Review on Advances in UV Spectroscopy. 2020. **12**(1): p. 47-51.
32. N.S. Nemeş, A.J.M.E.T.F. Negrea, and Applications, Infrared and Visible Spectroscopy: Fourier Transform Infrared Spectroscopy and Ultraviolet–Visible Spectroscopy. 2023. **1**: p. 163-200.
33. D.L. Pavia, G.M. Lampman, and G.S.J. Kriz, Introduction to organic laboratory techniques: a contemporary approach. 1976.
34. D. Harvey, *Modern analytical chemistry*. 2000: McGraw Hill.
35. J. Cazes, *Analytical instrumentation handbook*. 2004: CRC Press.
36. C. Adeeyinwo, et al., Basic calibration of UV/visible spectrophotometer. 2013. **2**(3): p. 247-251.
37. E. Pourbasheer, et al., Design of a novel optical sensor for determination of trace amounts of copper by UV–visible spectrophotometry in real samples. 2018. **32**(3): p. e4110.
38. A.A.A. Hassoni and A.S. Abbas. *Cloud point extraction for the determination of copper (II) by UV-visible spectrophotometry*. in *AIP Conference Proceedings*. 2022. AIP Publishing.
39. M.-B. Kime and D.J.C.E.C. Makgoale, Characterization of copper–cobalt ores and quantification of Cu2+, Co2+, Co3+, and Fe3+ in aqueous leachates using UV/Visible spectrophotometry. 2016. **203**(12): p. 1648-1655.
40. M.-h. Cui, et al., A novel UV-visible chemosensor based on the 8-hydroxyquinoline derivative for copper ion detection. 2015. **7**(10): p. 4252-4256.
41. J.i.J.A. Miura, Masking agents in the spectrophotometric determination of metal ions with 2-(5-bromo-2-pyridylazo)-5-diethylaminophenol and non-ionic surfactant. 1989. **114**(10): p. 1323-1329.
42. S.S. Hassan, et al., Determination of metformin in pharmaceutical preparations using potentiometry, spectrofluorimetry and UV–visible spectrophotometry. 1999. **378**(1-3): p. 299-311.
43. F. Zhou, et al., Determination of trace ions of cobalt and copper by UV–vis spectrometry in purification process of zinc hydrometallurgy. 2019. **184**: p. 227-233.
44. J.J. Pinto, et al., A simple and very sensitive spectrophotometric method for the direct determination of copper ions. 2002. **373**: p. 844-848.
45. T. Güray and Ü.D.J.J.o.t.C.S.o.P. UYSAL, Validated UV-Vis Spectrophotometric Method for the Determination of Copper using 2, 3, 4, 6/-Tetrahydroxy-3/-Sulfoazobenzene in Real Samples. 2018. **40**(3).
46. M.M. Hassan and A.F. Hussain. *Study of the spectrophotometric determination of Copper ion (I) by Michler's thioketone Reagent*. in *IOP Conference Series: Materials Science and Engineering*. 2020. IOP Publishing.
47. C. Kavitha, et al., Spectrophotometric determination of copper as copper piperazine. 2013. **8**: p. 205-209.
48. E. Chiyindiko, E.H. Langner, and J.J.E.A. Conradie, Electrochemical behaviour of copper (II) complexes containing 2-hydroxyphenones. 2022. **424**: p. 140629.
49. E. Chiyindiko, E.H. Langner, and J.J.M. Conradie, Spectroscopic behaviour of copper (II) complexes containing 2-hydroxyphenones. 2022. **27**(18): p. 6033.
50. E. Santoyo, S. Santoyo-Gutiérrez, and S.P.J.J.o.C.A. Verma, Trace analysis of heavy metals in groundwater samples by ion chromatography with post-column reaction and ultraviolet–visible detection. 2000. **884**(1-2): p. 229-241.
51. A. Timerbaev and G.J.J.o.C.A. Bonn, Complexation ion chromatography—an overview of developments and trends in trace metal analysis. 1993. **640**(1-2): p. 195-206.
52. N.J. Williams, et al., Possible steric control of the relative strength of chelation enhanced fluorescence for Zinc (II) compared to Cadmium (II): Metal ion complexing properties of Tris (2-quinolylmethyl) amine, a crystallographic, UV− Visible, and fluorometric study. 2009. **48**(4): p. 1407-1415.
53. M. Shakil Hossain, Determination of lead (pb) in trace amount using Ultraviolet-visible spectrophotometric method. 2011.
54. J. Mutembei, et al., Determination of heavy metals and nutrients in Rivers Naka and Irigu,

Chuka,(Kenya) using atomic absorption spectrometry and UV/visible spectrophotometry. 2014. **7**(11): p. 82-88.
55. W. Ruengsitagoon, A. Chisvert, and S.J.T. Liawruangrath, Flow injection spectrophotometric determination of lead using 1, 5-diphenylthiocarbazone in aqueous micellar. 2010. **81**(1-2): p. 709-713.
56. N. Rajesh, S.J.S.A.P.A.M. Manikandan, and B. Spectroscopy, Spectrophotometric determination of lead after preconcentration of its diphenylthiocarbazone complex on an Amberlite XAD-1180 column. 2008. **70**(4): p. 754-757.
57. M. Luconi, et al., Flow injection spectrophotometric analysis of lead in human saliva for monitoring environmental pollution. 2001. **54**(1): p. 45-52.
58. C. Okoye, et al., Simultaneous ultraviolet-visible (UV–VIS) spectrophotometric quantitative determination of Pb, Hg, Cd, As and Ni ions in aqueous solutions using cyanidin as a chromogenic reagent. 2013. **8**(3): p. 98-102.
59. Z.A. Khammas, A.A. Ghali, and K.H.J.I.J.C.S. Kadhim, Combined cloud-point extraction and spectrophotometric detection of lead and cadmium in honey samples using a new ligand. 2012. **10**(3): p. 1185-1204.
60. K.M. Elsherif, et al., Facile spectrophotometric determination of Cd (II) and Pb (II) using murexide reagent in mixed solvent system. 2022. **8**(4): p. 144-152.
61. H. Khan, M. Jamaluddin Ahmed, and M.J.S. Iqbal Bhanger, A simple spectrophotometric method for the determination of trace level lead in biological samples in the presence of aqueous micellar solutions. 2006. **20**(5-6): p. 285-297.
62. H.J.C.P. Cesur, Selective solid-phase extraction of Cu (II) using freshly precipitated lead diethyldithiocarbamate and its spectrophotometric determination. 2007. **61**: p. 342-347.
63. R. Dagnall, T. West, and P.J.T. Young, Determination of lead with 4-(2-pyridylazo)-resorcinol—I: Spectrophotometry and solvent extraction. 1965. **12**(6): p. 583-588.
64. Z. Marczenko and M. Balcerzak, *Separation, preconcentration and spectrophotometry in inorganic analysis*. 2000: Elsevier.
65. K. Matharu, et al., Selectivity enhancement of Arsenazo (III) reagent towards heavier lanthanides using polyaminocarboxylic acids: A spectrophotometric study. 2015. **145**: p. 165-175.
66. L.S.G. Teixeira, et al., Spectrophotometric determination of uranium using 2-(2-thiazolylazo)-p-cresol (TAC) in the presence of surfactants. 1999. **10**: p. 519-522.
67. A.R. Sekhar, et al., Porphyrin as a versatile visible-light-activatable organic/metal hybrid photoremovable protecting group. 2022. **13**(1): p. 3614.
68. D. Xu, et al., Simultaneous determination of traces amounts of cadmium, zinc, and cobalt based on UV–Vis spectrometry combined with wavelength selection and partial least squares regression. 2014. **123**: p. 430-435.
69. M.J. Ahmed and M.T.I.J.A.S. Chowdhury, A simple spectrophotometric method for the determination of cadmium in industrial, environmental, biological and soil samples using 5, 7-dibromo-8-hydroxyquinoline. 2004. **20**(6): p. 987-990.
70. K. Parikh, R. Patel, and K.J.E.-J.o.C. Patel, New spectrophotometric method for determination of cadmium. 2009. **6**(S1): p. S496-S500.
71. E.Y.J.S.A.P.A.M. Hashem and B. Spectroscopy, Spectrophotometric studies on the simultaneous determination of cadmium and mercury with 4-(2-pyridylazo)-resorcinol. 2002. **58**(7): p. 1401-1410.
72. B. Nagalaxmi, et al., Determination of trace amount of Cd (II) by using a chromogenic reagent diacetylmonoxime-3-amino-4-hydroxy benzoyl hydrazone (DMAHBH) with UV-visible spectrophotometry. 2015. **4**(2): p. 104-111.
73. A.A. Ensafi and Z.N.J.J.o.a.c. Isfahani, A simple optical sensor for cadmium ions assay in water samples using spectrophotometry. 2011. **66**: p. 151-157.
74. M.M. AL-Kishwan, M.A. AL-Daamy, and S.H. Kadhim. *Spectrophotometric determination of Cd (II) using reagent derived from unsubstituted imidazole*. in *AIP Conference Proceedings*. 2023. AIP Publishing.
75. S.G. Lee and H.S.J.B.o.t.K.C.S. Choe, Spectrophotometric determination of cadmium and copper with ammonium pyrrolodinedithiocarbamate in nonionic Tween 80 micellar media. 2001. **22**(5): p. 463-466.
76. Z. Ali, et al., Characterization of semiconductor CdS/Poly (vinyl alcohol) nanocomposites using ultraviolet/visible spectrophotometry. 2015. **2**: p. 17-29.
77. S. Karaderi, M. Bakla, and C.J.I.J.P.R.A.S. Mazı, Determination of UV-Vis Spectrophotometric Method of Metal Complexes Stoichiometry between Cu (II), Ca (II), Cd (II), Mg (II) and Zn (II) with Bupropion Hydrochloride. 2019. **8**: p. 1-9.
78. D. Oxspring, T. Maxwell, and W.J.A.c.a. Smyth, UV-visible spectrophotometric, adsorptive stripping voltammetric and capillary electrophoretic study of 2-(5′-bromo-2′-pyridylazo)-5-diethylaminophenol and its chelates with selected metal ions: application to the determination of Co (III) in vitamin B12. 1996. **323**(1-3): p. 97-105.
79. G. Mohamed, et al., Extractive spectrophotometric method for determination of cadmium (II) in different water sources. 2015. **212**: p. 517-523.
80. M. Eskandarpour, et al., Developing a highly selective method for preconcentration and determination of cobalt in water and nut samples using 1-(2-pyridylazo)-2-naphthol and UV–visible spectroscopy. 2020. **100**(5): p. 2272-2279.
81. B.M. Weckhuysen, Ultraviolet-visible spectroscopy. 2004.
82. D. Harvey, *Spaces of hope*. Vol. 7. 2000: Univ of California Press.
83. P.D. Sethi, *Quantitative analysis of drugs in pharmaceutical formulations*. 2008: CBS.
84. A. Ferdowsi and H.J.T.o.N.M.S.o.C. Yoozbashizadeh, Process optimization and kinetics for leaching of cerium, lanthanum and neodymium elements from iron ore waste's apatite by nitric acid. 2017. **27**(2): p. 420-428.
85. H.M. Hassan, et al., A novel and potential chemical sensor for effective monitoring of Fe (II) ion in corrosion systems of water samples. 2020. **154**: p. 104578.
86. S. Pepper, et al., Determination of ferrous and ferric iron in aqueous biological solutions. 2010. **663**(2): p. 172-177.
87. X. Cai, et al., Novel Pb2+ Ion Imprinted Polymers Based on Ionic Interaction via Synergy of Dual Functional Monomers for Selective Solid-Phase Extraction

of Pb2+ in Water Samples. *ACS Applied Materials & Interfaces*, 2014. **6**(1): p. 305-313.
88. E.Y. Frag, N.A. Abd El-Ghany, and M.A.E.J.J.o.E.C. Fattah, Physico-chemical properties and characterization of iron (II) electrochemical sensor based on carbon paste electrode modified with novel antimicrobial Carboxymethyl chitosan-graft-poly (1-cyanoethanoyl-4-acryloyl-thiosemcarbazide) copolymers. 2018. **808**: p. 266-277.
89. H. Xie, et al., Rapid detection of iron ore grades based on Fractional-order derivative spectroscopy and machine learning. 2023.
90. A.S. Farhood and D.N.J.분. Taha, A new merging-zone flow injection system for the quantification of ferrous and ferric ions in aqueous solution and sludge of wastewater. 2022. **35**(5): p. 218-227.
91. Y. Du, et al., Stalk-derived carbon dots as nanosensors for Fe3+ ions detection and biological cell imaging. 2023. **11**: p. 1187632.
92. F. Zhou, et al., Simultaneous determination of trace metal ions in industrial wastewater based on UV–vis spectrometry. 2019. **176**: p. 512-517.
93. F. Cheng, et al., A direct and rapid method for determination of total iron in environmental samples and hydrometallurgy using UV–Vis spectrophotometry. 2022. **179**: p. 107478.
94. O. Turkoglu and M.J.J.o.t.C.C.S. Soylak, Spectrophotometric determination of copper in natural waters and pharmaceutical samples with chloro (phenyl) glyoxime. 2005. **52**(3): p. 575-579.
95. N. Nik-Abdul-Ghani, et al., Study of graphene oxide-polymer nanocomposite (GPN) adsorptive membrane for lead removal from wastewater. 2021. **5**: p. 3620-3636.